

New data in the interpretation of the geology and morphology of Maddur area, Andhra Pradesh through Remote Sensing – T. Vani, UCESS, University of Hyderabad, Present Address: Flat No.101, Plot No.100, Sudharshan nagar Colony, Lingampally, Hyderabad – 500019(E-mail: turlapativani@yahoo.com)

Maddur and its environs in Andhra Pradesh, India are well known as the second largest kimberlite field in eastern Dharwar craton with ~ 34 pipes. Dykes and domal structures observed in the remote sensing images show the permeable nature of the rocks in the area. The northwesterly plunging synclinorium folds in the metasedimentary rocks and a number of fractures in the granitic rocks delineated from the LISS III (Fig. 1) image reveal their brittle nature.

Lineaments interpreted from both gravity and magnetic data and the faults/fractures inferred from the remote sensing data show corroboration with the geological trends. Structural interpretation of remote sensing data including geophysical data is very effective in delineating faults, fractures and potential kimberlite zones (Fig. 2).

Geology

Maddur kimberlite field is one of the major kimberlite fields in the eastern Dharwar craton. The study area mainly consists of biotite granite, migmatite gneiss, small patches of Deccan traps in the NW region along with long narrow patches of schistose rocks. Number of faults/fractures are marked on the geological map in NW-SE, NE-SW, E-W and N-S directions (Rao et al. 1999; Vani et al. in press). NW-SE trending faults/fractures appear to be following the Dharwarian trend. Known kimberlite pipes are differentiated into three major clusters (Fig. 2). These pipes are subsisting along the faults/fractures, at the intersection of faults/fractures and the contacts of different lithological units.

Methodology

IRS P6 satellite data of LISS III sensor, covering an area of ~ 4700 sq km is used for the interpretation.

Remote sensing data

Patterns, shapes, tonal and textural contrasts and drainage patterns are used to identify various structural and

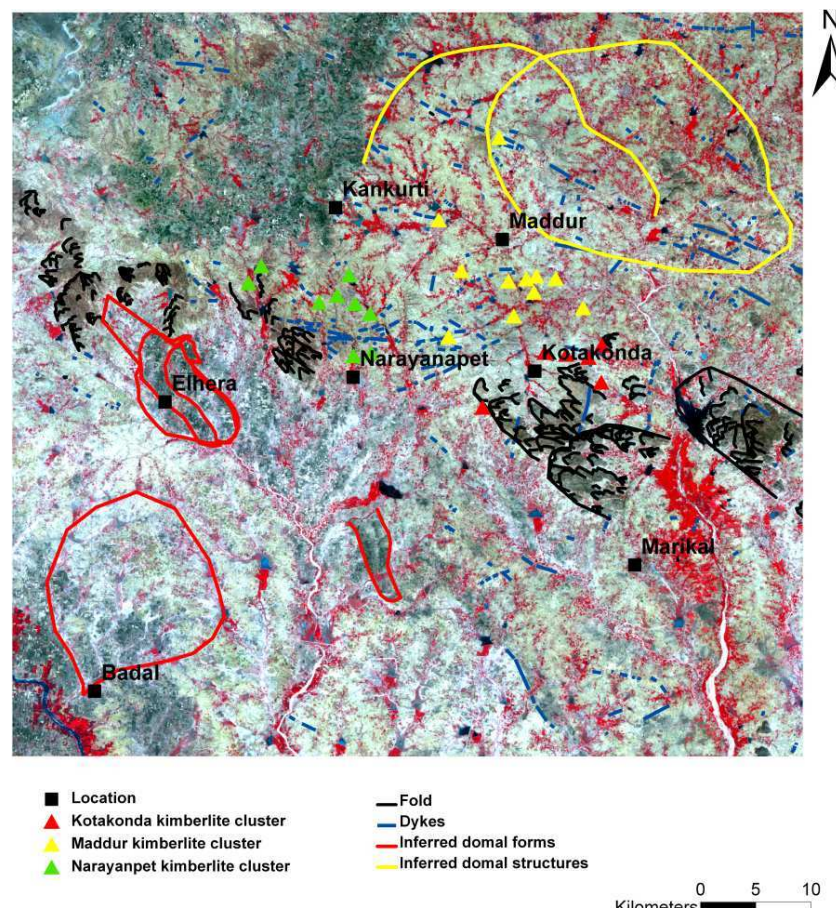


Fig.1. LISS III image of Maddur region with inferred domal structures and folds (map is prepared on 1:100,000 scale, but the structural features are identified on 1:50,000 scale).

geomorphological features in the LISS III image. Central and NE portions of the image indicate the highly disturbed massive rocks with brittle nature. Arc type massive granites are exposed in the northeastern part of the study area. Pediplaination is observed over weathered rocks on the southwestern side due to the intensely dissected drainage pattern with number of consequent streams. Inferred structural and morphic features are discussed below.

Faults

Based on drainage patterns, displacements and cut-offs of strata, NW-SE, E-W and NE-SW trending faults with

varying lengths between ~ 45 and 74 km have been inferred (Fig. 2). These extensive faults may indicate their deep seated nature and are likely to have acted as favourable conduits for emplacement of the kimberlite pipes. An apparent E-W cut of strata in the western section of the eastern end of the W-E lineament (AB of Fig 2) is clearly observed close to north of Narayanpet. This E-W extending fault along with NE-SW trending minor tensional fractures played an important role in the emplacement of Maddur and Kotakonda pipes (Rao et al. 1999). This major fault also corroborates with the inferred geophysical lineament and with slight offset from the fault traced from

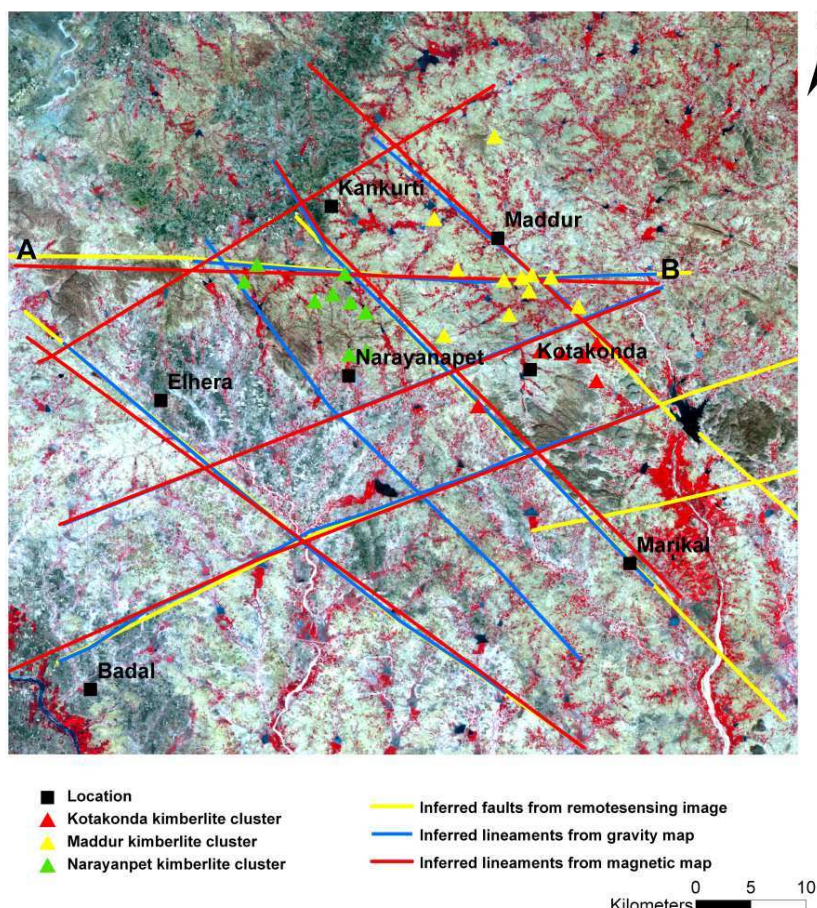


Fig 2. LISS III image of Maddur region with inferred lineaments from gravity and magnetic data and inferred faults from remote sensing image (map is prepared on 1:100,000 scale, but the structural features are identified on 1:50,000 scale).

the geological data. It is also possible that some of the faults may be shear zones which can only be confirmed by field study.

Fractures

In addition to the faults, a number of fractures are also inferred in the study area indicating the structural disturbances the area has undergone. Based on some of the radial drainage patterns a few curvilinear fractures are also observed on the image. It is possible that some of the faults identified may be petering out as fractures at their extremities.

Dykes

Number of dykes trending in all directions indicates the permeable nature of the sediments in the area. Numerous small-scale dykes are delineated between the two major NW-SE plunging synclinoriums (Fig 1). It appears that major tectonic events

played an important role in the disposition and alignment of the dykes. Depending on colour contrast, a few quartz reefs can be differentiated from the other dykes on the NW corner of the map.

Folds

Cluster of folds, plunging in NW direction in the younger granitic gneiss follow the trend of the synclinorium (Fig. 1). Two sets of folds are observed. They might have been developed due to different geological ages. It is also observed that the different synclinoriums appeared to be in an en echelon pattern. This may be the result of step wise faulting in E-W and NW-SE directions. Most of the known Narayananpet and Kotakonda pipes are subsisting over the folded strata.

Drainage pattern

Drainage pattern reflects the nature of

lithology and structure of the given area. Dendritic pattern is observed near NE of Narayananpet, indicating the presence of uniform massive granitic rock and the same pattern can be observed over the folded strata. Rectangular drainage pattern in SW corner near Badal village is likely to indicate the presence of two sets of jointing (at right angles) in the rocks of nearly uniform composition with approximately uniform resistance to erosion.

Most of the consequent streams follow N-S and NW-SE directions following the slope towards southern side in conformity with slope of the terrain in those directions. Radial pattern is observed near Kankurthi village. This is usually associated with domal structures (Fig. 1).

Domal forms

A few domal forms have been marked from LISS III data depending on the radial drainage pattern and other morphological features in the northern side of Maddur as shown in Fig. 1. In the NW, these forms have been delineated mainly depending on the tonal and texture contrasts. Near Elhera village, below the major E-W fault a small domal form has been delineated and it appears to be filled with the material transported from the Deccan traps.

Domal structures

These have been drawn mainly taking into consideration of partially anomalous drainage trends along with curvilinear trends (Fig. 1). Their significance is not known but they may be indicating the presence of subsurface intrusive plutons. Ramadass et al. (2006) identified few domal forms within which known kimberlite pipes occur. It was suggested that there might be an association between kimberlite pipes and domal forms. In the present study a few domal forms/structures have been identified in the images. The pattern of gravity anomalies reported by Sreerama Murthy et al. (1999) also look similar to these domal structures.

Geophysical data

Gravity and magnetic data (Vani et al., *in press*) reveal the subsurface structure depending on the density and susceptibility contrasts respectively. These maps clearly

brought out the hidden long and wide schist belts, which appears to be separating the migmatite gneiss and biotite granite. Geophysical lineaments are inferred depending on the deflections, offsets, terminations and linearity of the contours obtained from the geophysical data. NW-SE, NE-SW & E-W lineaments are inferred from both gravity and magnetic maps including the bounding lineaments of the schist belt (Fig. 2). These lineaments are corroborating with surface inferred faults from the satellite image.

Potential zones of kimberlite pipes obtained by Euler deconvolution method (Vani et al., *in press*) are falling in and around inferred partial domes.

Conclusions

Various inferred structural and morphological features such as faults,

fractures, dykes, domal forms and structures traced from the LISS III images show the complex nature of the surface. Integration of geophysical, geological and remote sensing data brought out the (a) six major faults including fractures (b) Intersections of faults/lineaments & domal structures are likely loci for potential kimberlite zones identified from the Euler deconvolution method of potential field data.

Acknowledgements: I greatly acknowledge Indo-US S&T forum and Kaigala Suryachandraraao Trust for financial assistance. My respectful thanks to Prof. R. Vaidyanadhan, Prof. K.V.Subbarao and Sri M.V.R.K.Rao for their help; APSRAC and in particular Dr. V. Raghu for discussions; and to an anonymous referee for valuable suggestions.

References

- RAMADASS, G., HIMABINDU, D. AND VEERAIAH, B. (2006) Morphostructural prognostication of kimberlites in parts of eastern Dharwar craton: Inferences from remotesensing and gravity signatures. Jour. of the Indian Society of Remotesensing, v.34, no.2, pp.11 -121.
 RAO, K.R.P., REDDY, T.A.K., RAO, K.V.S., RAO, K.S.B. AND RAO, N.V. (1999) Geology, Petrology and Geochemistry of Narayanpet kimberlite field in Andhra Pradesh and Karnataka. Jour. of Geol. Soc. of India, v.52, pp.663-676.
 SREERAMA MURTHY, N., ANANDA REDDY, R., RAO, M.V.R.K., SUNDER RAJ, B., MURTHY, N.V.S. AND VITTAL RAO, K.P.R. (1999) A new kimberlite discovery from a structural elucidation of gravity data, Maddur – Narayanpet field, Mahabubnagar district, Andhra Pradesh. Jour. of Geophy., v. 20, no.1, pp.3-13.

A Perovskitic Lower Mantle Inferred from High-pressure, High-temperature Sound Velocity Data by Motohiko Murakami, Yasuo Ohishi, Naohisa Hirao and Kei Hirose

The above paper published in *Nature*, v.485, pp.90-94, 03 May 2012, the authors determine the shear-wave velocities for silicate perovskite and ferropericlase under the pressure and temperature conditions of the deep lower mantle using Brillouin scattering spectroscopy. The mineralogical

model that provides the best fit to a global seismic velocity profile indicates that perovskite constitutes more than 93 per cent by volume of the lower mantle, which is a much higher proportion than that predicted by the conventional peridotitic mantle model. It suggests that the lower mantle is

enriched in silicon relative to the upper mantle, which is consistent with the chondritic Earth model. Such chemical stratification implies layered-mantle convection with limited mass transport between the upper and the lower mantle.

Deposition of 1.88-billion-year-old Iron Formations as a Consequence of Rapid Crustal Growth by Birger Rasmussen, Ian R. Fletcher, Andrey Bekker, Janet R. Muhling, Courtney J. Gregory and Alan M. Thorne

The above paper published in *Nature*, v.484, pp.498-501, 26 April 2012 may be of interest to researchers who are involved in the study of iron formations.

Iron formations are chemical sedimentary rocks comprising layers of iron-rich and silica-rich minerals whose deposition requires anoxic and iron-rich (ferruginous) sea water. Their demise after the rise in atmospheric oxygen by 2.32 billion years (Gyr) ago has been attributed to the removal of dissolved iron through progressive oxidation or sulphidation of the deep ocean. Therefore, a sudden return of voluminous iron formations nearly 500 million years later poses an apparent

conundrum. Here the authors date zircons in tuff layers to show that iron formations in the Frere Formation of Western Australia are about 1.88 Gyr old, indicating that the deposition of iron formations from two disparate cratons was coeval and probably reflects global ocean chemistry. The sudden reappearance of major iron formations at 1.88 Gyr ago—contemporaneous with peaks in global mafic–ultramafic magmatism, juvenile continental and oceanic crust formation, mantle depletion and volcanogenic massive sulphide formation—suggests deposition of iron formations as a consequence of major mantle activity and rapid crustal growth. The findings support

the idea that enhanced submarine volcanism and hydrothermal activity linked to a peak in mantle melting released large volumes of ferrous iron and other reductants that overwhelmed the sulphate and oxygen reservoirs of the ocean, decoupling atmospheric and seawater redox states, and causing the return of widespread ferruginous conditions. Iron formations formed on clastic-starved coastal shelves where dissolved iron upwelled and mixed with oxygenated surface water. The disappearance of iron formations after this event may reflect waning mafic–ultramafic magmatism and a diminished flux of hydrothermal iron relative to seawater oxidants.